Hybrid Oligomer Duplexes Formed with Phosphorothioate DNAs: CD Spectra and Melting Temperatures of S-DNA·RNA Hybrids Are Sequence-Dependent but Consistent with Similar Heteronomous Conformations†

Gihan M. Hashem, Lanhuong Pham, Marilyn R. Vaughan, and Donald M. Gray*

Program in Molecular and Cell Biology, Mail Stop FO31, The University of Texas at Dallas, Box 830688, Richardson, Texas 75083-0688

Received June 6, 1997; Revised Manuscript Received October 27, 1997⊗

ABSTRACT: Knowledge of the relative stabilities of S-DNA·RNA hybrids of different sequences is important for choosing RNA targets for hybridization with antisense phosphorothioate oligodeoxyribonucleotides (S-DNAs). It is also important to know how hybrid secondary structure varies with sequence, since different structures could influence thermal stability and the activity of RNase H. Our approach has been to study relatively simple sequences consisting of repeating di-, tri-, and tetranucleotides, which allow the maximum resolution of nearest-neighbor effects. Circular dichroism (CD) spectra and melting temperatures were acquired for 16 hybrid sequences that could be formed by mixing S-DNA and RNA oligomers of 24 nucleotides in length. CD spectra of S-DNA·RNA hybrids were sequence-dependent and were similar to those of analogous unmodified hybrids. From singular value decomposition, the major CD spectral component was like that of the A-conformation. Three nearest-neighbor relationships among the hybrid CD spectra were in as good agreement as are such relationships among spectra of duplex RNAs. T_m values ranged from 44.1 °C for S-d(ACT)$_8$·r(AGU)$_8$ to 66.6 °C for S-d(CCT)$_8$·r(AGG)$_8$ (in 0.15 M K^+, phosphate buffer, pH 7). The S-DNA·RNA hybrids had a sequence-dependence of melting temperatures that was approximately the same as that calculated using published data for normal DNA·RNA hybrids [Sugimoto, N., Nakano, S., Katoh, M., Matsumura, A., Nakamuta, H., Ohmichi, T.,Yoneyama, M., & Sasaki, M. (1995) *Biochemistry 34*, 11211−11216]. In general, sequence-dependent CD spectra and T_m values of S-DNA·RNA hybrids appear to reflect the unique nearest-neighbor interactions of adjacent base pairs, where the S-DNA and RNA strands are in different, but relatively uniform, conformations.

Interest in the use of oligodeoxyribonucleotides as antisense drugs stems from work by Zamecnik & Stephenson (1978; and Stephenson & Zamecnik, 1978), who demonstrated that the replication of Rous sarcoma virus can be inhibited with the addition of a DNA oligomer complementary to viral mRNA in infected cells. The formation of DNA·mRNA hybrids can be used to control gene expression by the inhibition of splicing, by the inhibition of the steps of translation, or by activation of RNase H leading to degradation of the mRNA (Agrawal et al., 1990). The successful use of an antisense DNA (complementary to an mRNA sequence) as a therapeutic agent requires that the DNA have desirable features such as resistance to cellular nucleases and the ability to activate RNase H when hybridized to mRNA. Among the many chemical modifications that have been introduced, one of the most successful has been the substitution (nonstereospecifically) of sulfur for one of the phosphodioxy nonbridge backbone oxygens to give a phosphorothioated DNA, S-DNA[1] (Stein et al., 1988; Stein & Cheng, 1993; Baum, 1994; Wagner, 1994; Cohen & Hogan, 1994; Gura, 1995; Gutierrez et al., 1997). S-DNAs are among the most important in the first generation of antisense DNA drugs, with 12 phosphorothioate oligonucleotides having progressed to the point of clinical trials (Matteucci & Wagner, 1996). Other chemical modifications, such as 2′-*O*-alkyl modifications, increase the stability of antisense S-DNAs, but such modifications reduce RNase H sensitivity. For this reason, chimeric antisense S-DNAs that combine 2′-*O*-alkyl phosphorothioates (to give stability) and a minimum of five simple phosphorothiate nucleotides (to retain RNase H sensitivity) have been advocated and have been shown to be effective in cells (Monia et al., 1993). Therefore, it seems likely that phosphorothioates will remain a focus of antisense technology.

Cellular uptake of S-DNA oligos has been well documented (Iversen et al., 1992; Politz et al., 1997; Thierry & Dritschilo, 1992; Temsamani et al.,1994; Crooke et al., 1995). Gray et al. (1997) compared the uptake of S-DNA oligomers with the uptake of peptide nucleic acids and of 3′-alkylamino, 2-*O*-methyl, and methylphosphonate DNAs in multiple cell lines. They demonstrated active cellular uptake of all the

† This work was supported by Cytoclonal Pharmaceutics, Inc., of Dallas, TX, the Texas Advanced Technology Program under Grant 9741-036, and Grant AT-503 from the Robert A. Welch Foundation.
⊗ Abstract published in *Advance ACS Abstracts,* December 15, 1997.

[1] Abbreviations: CD, circular dichroism; DEPC, diethyl pyrocarbonate; dsDNA, double-stranded DNA; dsRNA, double-stranded RNA; HPLC, high performance liquid chromatography, %H, percent hyperchromicity at 260 nm; OD, optical density; *R*, gas constant of 1.987 cal/(K mol); RMS, root mean square; S-DNA oligomer, oligomer of phosphorothioated deoxyribonucleotides; SVD, singular value decomposition; T_m, melting temperature.

S0006-2960(97)01355-X CCC: $15.00
Published on Web 01/06/1998

analogs within 1−3 h, but the intracellular accumulation of S-DNA oligomers exceeded that of the other analogs by 9−24 h. Accumulation of S-DNA oligomers in the nucleus was significant, being about 25% of the total uptake.

Properties of S-DNA oligomers that remain to be fully understood include their ability to act in a non-sequence-specific manner, due to their potential to bind to proteins such as growth factors and receptors (Brown et al., 1994; Stein, 1995; Khaled et al., 1996) and their ability to activate some transcription factors (Perez et al., 1994). The phosphorothioate substitution also reduces the stability of S-DNA·RNA relative to normal DNA·RNA hybrids. Nevertheless, there are many examples of a sequence specific antisense effect of S-DNA oligomers, as illustrated by the work of Maltese et al. (1995) and Dean et al. (1996).

To optimize the selection of antisense DNA oligomers, it is important to be able to compare the hybridization efficiencies of hundreds of possible antisense sequences paired with their respective target RNA sequences. One of the basic criteria for predicting the efficiency of the antisense effect is the thermodynamic stability of the DNA·RNA hybrids that are formed. Stull et al. (1992) showed that, for S-DNA oligomers of the same length, an estimate of the free energy of duplex formation using data for dsDNAs could be correlated with antisense effectiveness. However, thermodynamic data for dsDNAs or dsRNAs do not provide the best predictions of DNA·RNA hybrid stability, since there are 16 different nearest-neighbor base pairs in hybrids but only 10 different types of nearest-neighbor base pairs in a duplex DNA or RNA. The distribution of purines and pyrimidines on the DNA and RNA strands is itself of importance, hybrids that are rich in r(purine)·d(pyrimidine) sequences being more stable than hybrids that have d(purine)·r(pyrimidine) sequences (Roberts & Crothers, 1992; Ratmeyer et al., 1994; Hung et al., 1994; Lesnik & Freier, 1995; Gyi et al., 1996). Sugimoto et al. (1995) further showed, from measurements on 64 sequences of 5 to 12 base pairs in length, that the different types of nearest-neighbors do influence the thermodynamic parameters of DNA·RNA hybrids. As customary for studies of the thermodynamic parameters of dsDNA and dsRNA oligomers (Breslauer et al., 1986; Freier et al., 1986; SantaLucia, 1996; Sugimoto et al., 1996; Allawi & SantaLucia, 1997), the thermodynamic parameters were measured in the presence of 1 M NaCl. The 16 S-DNA·RNA hybrids in the present paper have melting temperatures that vary over a 22.5 °C range, at a physiological cation concentration of 0.15 M K^+. The sequence-dependence of melting temperatures of the S-DNA·RNA hybrids at this salt concentration is reflected in the published thermodynamic parameters for normal DNA·RNA hybrids in 1 M NaCl.

Hybrids in solvated or highly hydrated conditions are not in simple A conformations. Poly[r(A)·d(T)], poly[d(A)·r(U)], and poly[d(I)·r(C)] in hydrated fibers were found to have a heteronomous structure, in which the DNA and RNA strands have C2′-endo and C3′-endo sugars, respectively (Zimmerman & Pfeiffer, 1981; Arnott et al., 1986). Hybrids in solution are also heteronomous in sugar conformation, as shown by NMR and Raman spectroscopies (Benevides et al., 1986; González et al., 1994, 1995; Gyi et al., 1996; Nishizaki et al., 1996; Salazar et al., 1996; Rice & Gao, 1997). The two DNA·RNA hybrids in the NMR studies by González et al. (1994, 1995) each had one phosphorothioate linkage, one of R and one of S chirality. The sulfur atoms were accommodated without changes in the heteronomous structures. Molecular dynamics simulations indicated that the DNA strand may be in equilibrium between the two types of sugar conformation and may be more flexible than pure DNA or RNA. As shown by Nishizaki et al. (1996), short hybrid segments of four base pairs are heteronomous but differ in minor groove widths when within or at the ends of dsDNA regions.

CD spectroscopy has been widely used to characterize nucleic acids of the A and B conformations and of hybrids with normal and modified DNA strands (Gray & Ratliff, 1975; Gray et al., 1981; Steely et al., 1986; Hall & McLaughlin, 1991; Callahan et al., 1991; Roberts & Crothers, 1992; Hung et al., 1994; Johnson, 1994; Ratmeyer et al., 1994; Gray et al., 1995; Lesnik & Freier, 1995; Sugimoto et al., 1995; Gyi et al., 1996; Ding et al., 1996). The spectra of DNA·RNA hybrids are sequence-dependent, even for sequences such as poly[d(AC)·r(GU)] and poly[r(AC)·d(GT)] that have similar melting temperatures (Gray & Ratliff, 1975). On the other hand, the qualitatively different spectra of r(purine)·d(pyrimidine) and d(purine)·r(pyrimidine) hybrid sequences are correlated with different stabilities, the former being more thermostable (Roberts & Crothers, 1992; Hung et al., 1994; Ratmeyer et al., 1994; Lesnik & Freier, 1995; Gyi et al., 1996). Gyi et al. (1996) compared the thermodynamics, CD spectra, and NMR data for a set of four purine·pyrimidine duplexes, dsDNA, dsRNA, and two hybrids, each 10 base pairs long. Differences in CD spectra and stabilities of the hybrids were related to differences in NMR spectra. The results were interpreted as indicating that the two hybrids have different DNA strand conformations and that the DNA strand of the r(purine)·d(pyrimidine) hybrid was the more flexible. In work by Lesnik & Freier (1995), the free energy of hybrid formation (relative to the dsRNA) was correlated with differences in electrophoretic mobility (except for sequences with A-tracts) and with the negative 210 nm CD band magnitude, expressed as the difference in the band for dsRNA minus hybrid (relative to the difference for dsRNA minus dsDNA). If the CD spectra do indicate differences in hybrid conformation, this could be an important indicator of not only stability but also RNAse H activity. Lima & Crooke (1997) specifically suggested that RNAse H1 activity may be enhanced for hybrids formed from S-DNAs that are pyrimidine rich, if these are closer to the A-conformation in their secondary structure. Oda et al. (1993) used CD spectroscopy to demonstrate that the conformations of DNA·RNA hybrids 11 and 22 base pairs long are altered on binding to *E. coli* RNase H1, apparently to be closer to the A-conformation since a negative band at 288 nm appeared upon binding. Therefore, a key question is whether sequence-dependent CD spectral features for hybrids, especially those with S-DNAs, do imply substantial differences in hybrid secondary structure.

In order to predict the value of a nearest-neighbor property of a hybrid sequence, the values must be known for a minimum of 13 sequences, if the sequences are long enough that end effects may be neglected and if they are all in the same conformation. That is, each type of nearest-neighbor must make the same contribution in all sequence contexts. The minimum set of sequences must also have linearly

Table 1: Sources and Extinction Coefficients of 16 Complementary Single-Stranded S-DNA and RNA Oligomers Used to Make Hybrid Duplexes

	S-DNA			RNA		
	sequence	source	ϵ_{260}[a]	sequence	source	ϵ_{260}[a]
			67% A + T(U)			
1	S-d(AGT)$_8$	*c*	12 070[b]	r(ACU)$_8$	*c*	10 010
2	S-d(CTT)$_8$	*d*	7 950	r(AAG)$_8$	*d*	12 030
3	S-d(ATC)$_8$	*c*	9 680	r(GAU)$_8$	*c*	11 140
4	S-d(ACT)$_8$	*c*	9 550	r(AGU)$_8$	*c*	11 630
			50% A + T(U)			
5	S-d(AG)$_{12}$	*c, d*	13 750[b]	r(CU)$_{12}$	*c, d*	8 360
6	S-d(GT)$_{12}$	*c, d*	9 550	r(AC)$_{12}$	*c, d*	9 940
7	S-d(AC)$_{12}$	*c, d*	9 940	r(GU)$_{12}$	*c, d*	10 240
8	S-d(CT)$_{12}$	*c, d*	7 660	r(AG)$_{12}$	*c, d*	12 030
9	S-d(AAGG)$_6$	*c*	13 750[b]	r(CCUU)$_6$	*c*	8 540
10	S-d(AACG)$_6$	*c*	12 640[b]	r(CGUU)$_6$	*c*	10 040[b]
11	S-d(AAGC)$_6$	*c*	12 610[b]	r(GCUU)$_6$	*c*	10 040[b]
12	S-d(AACC)$_6$	*c*	9 850	r(GGUU)$_6$	*c*	10 330
			33% A + T(U)			
13	S-d(AGC)$_8$	*d*	11 700[b]	r(GCU)$_8$	*d*	9 990[b]
14	S-d(GCT)$_8$	*d*	9 490[b]	r(AGC)$_8$	*d*	11 700[b]
15	S-d(CCT)$_8$	*d*	7 970[b]	r(AGG)$_8$	*d*	13 220[b]
16	S-d(ACG)$_8$	*c*	11 700[b]	r(CGU)$_8$	*c*	9 990[b]

[a] Calculated from the ϵ_{260} values of the monomers and dimers at 20 °C as in Gray et al. (1995), except as noted. [b] Calculated for the oligomer at 90 °C (for cases where the oligomer may not have been single-stranded at 20 °C) from the average ϵ_{260} values of the monomers. [c] Synthesized by Oligos, Etc., Inc. [d] Synthesized at Los Alamos National Laboratory by Dr. R. L. Ratliff.

independent combinations of nearest-neighbors, so that no one nearest-neighbor combination may be derived by a linear combination of the others (Gray & Tinoco, 1970). The present work is on hybrids formed with phosphorothioate DNA oligomers 24 nucleotides long to minimize end effects. Sixteen sequences were formed that encompass an independent set of thirteen, plus three more that can be used in nearest-neighbor calculations of properties. Since circular dichroism is approximately a nearest-neighbor effect (Gray et al., 1981), a nearest-neighbor comparison of spectra is one indication of conformational uniformity. In the present work, CD spectroscopy data of a subset of 12 of the S-DNA·RNA hybrids were consistent with the hybrids being in essentially the same heteronomous conformation.

MATERIALS AND METHODS

Samples. The oligomers used in this study were S-DNA oligomers and unmodified ribonucleotides (RNA oligomers) that were 24 nucleotides long. The sequences are given in Table 1. The oligomers were either prepared by Dr. Robert Ratliff (Los Alamos National Laboratory, Los Alamos, NM) or purchased from Oligos, Etc., Inc. (Wilsonville, OR). Ten of the S-DNA oligomers were HPLC purified by Oligos, Etc. After experiments were completed, eight of the oligomers (two S-DNAs that were HPLC purified, two S-DNAs from Los Alamos National Laboratory, and four RNAs from Oligos, Etc.) were subjected to gel electrophoresis (20% polyacrylamide, 8 M urea), stained with SYBR Green II (Molecular Probes, Inc., Eugene OR), and digitized using a Biophonics Model 2000i Gel Print System. The oligomers electrophoresed as one major band with a few minor bands of truncated products. The major bands for the DNAs and three of the RNAs contained over 90% of the material, while the major bands for the other RNA contained 85% of the material. To inhibit RNase degradation, single stranded S-DNA and RNA oligomers were dissolved in water treated with DEPC (diethyl pyrocarbonate). The procedure was to add 0.1% (v/v) DEPC to distilled, deionized water, hold at room temperature overnight, and autoclave for 15 min to remove traces of DEPC that can increase absorbance of the buffer or modify purine residues in RNA. Oligonucleotides were stored in 200 μL aliquots at −20 °C. For a mixing experiment, an aliquot of 200 μL was thawed, and the single strands were diluted in 2 mM K^+(phosphate buffer, pH 7.0) for a determination of concentration using absorbance measurements together with extinction coefficients at 260 nm. Extinction coefficient for single-stranded oligomers at 20 °C were calculated from the extinction coefficients of the monomers and dimers (Gray et al., 1995), using the nearest neighbor approximation. It was assumed that extinction coefficients for S-DNAs were the same as for unmodified DNAs. If an oligomer possessed intrastrand structure according to preliminary CD and T_m measurements, then the oligomer concentration was determined from its absorbance at 90 °C and the average of the monomer extinction coefficients at 260 nm (Gray et al., 1995). See Table 1.

For mixing experiments, complementary single strands were prepared in 0.15 M K^+ (phosphate buffer, pH 7.0) to have the same molar nucleotide concentrations, which ranged from 5 to 6 × 10^{-5} M nucleotides (2.1 to 2.5 μM in strands) for different strand pairs. Additional experiments were done with samples prepared in 0.15 M Na^+ (phosphate buffer, pH 7.0) to investigate the effect of Na^+ *versus* K^+ cations on the CD of single strands and duplexes and on T_m values. To test the effect of a divalent cation, four samples were also studied in the presence of 2 mM Mg^{2+}. Small aliquots of 0.2 M $MgCl_2$ were added to two hybrids in 0.15 M K^+ and to two hybrids in 0.15 M Na^+ to give a final concentration of 2 mM Mg^{2+}. The Mg^{2+} concentration was kept low since precipitates formed during heating in the presence of 20 mM Mg^{2+}. Absorbance and CD measurements were taken before and after the addition of Mg^{2+} ions, and there was no spectral evidence for precipitation during heating in 2 mM Mg^{2+}. The effect of higher cation concentration on the T_m was explored with samples hybridized in 0.15 M K^+ (phosphate buffer, pH 7.0) to which 4 M NaCl and water were added to give a total cation concentration of 1.01 M (0.90 M Na^+ plus 0.11 M K^+).

Mixtures. Complementary oligomers were mixed at the following S-DNA:RNA ratios; 100:0, 80:20, 67:33, 60:40, 50:50, 40:60, 33:67, 20:80, and 0:100. Mixtures were allowed to equilibrate at room temperature for 2 h or at 4 °C for 24 h before measurements of absorbance, CD, and melting profiles. The two equilibration treatments gave equivalent CD and OD measurements. Two of the mixtures (Nos. 15 and 16 in Table 1) required heating to allow duplex formation, due to competing intrastrand structure in one or both of the single strands; these samples were heated by incubation at 90 °C for 90 s and were then allowed to cool slowly at room temperature for 24 to 48 h before measurements.

Instrumentation. Absorbance readings were taken with a Cary-Varian Model 118 or an Olis-modified Cary 14 spectrophotometer, and CD measurements were taken with a Jasco Model J500A or J710 spectropolarimeter. Sample

chambers of all the instruments were temperature-controlled with Neslab E-111 water baths. Except during melting experiments, spectra were taken at 20 °C. Sample path lengths were 1 cm. CD spectra were taken from 320 to 200 nm, data being collected at 0.1 nm intervals at scan speeds of 10 and 40 nm/min, respectively, in the J500 and J710. Spectra from the J710 were the averages of four repeat scans. After baseline subtraction, data from the J500 were saved every 1 nm and smoothed using a 13-point quadratic-cubic least squares algorithm (Savitzky & Golay, 1964), and data from the J710 were smoothed using the Fourier transform algorithm provided by Jasco. Since some spectra became progressively noisy below 210 nm, they were truncated at 205 nm. Spectral measurements made at 20 °C were used to plot mixing curves to evaluate whether each S-DNA·RNA pair indeed formed a hybrid duplex. When a duplex was formed, the mixing curves exhibited break points close to the 50:50 ratio of the mixed strands.

Melting Profiles. Melting profiles (OD versus temperature) were obtained for the 50:50 mixtures containing the duplexes. The OD (260 nm) was monitored in the Olis-modified Cary 14 as the temperature was increased from 20 to 90 °C in increments of 1 °C. Samples were incubated for 3 min at each target temperature to allow for equilibration before taking OD readings, which were then corrected for sample volume expansion. T_m values were obtained from the first derivatives of the melting profiles, using a 13-point quintic-sexic first derivative procedure (Savitzky & Golay, 1964). Temperatures were reproducible to ±0.1 °C and were calibrated to be accurate to ±0.5 °C. Samples were weighed before and after each melting profile to determine the amount of evaporation, which was usually less than 1%.

Singular Value Decomposition. A singular value decomposition routine following Press *et al*. (1992) was applied to a 116 column × 16 row matrix (**A**) of spectra (from 205 to 320 nm, in 1-nm intervals) of the 16 sequences studied. Using the notation of Henry & Hofrichter (1992) and Johnson (1992), $\mathbf{A} = \mathbf{U}\,\mathbf{S}\,\mathbf{V^t}$. The first and second columns of matrix **U** times the negative of the first and second singular values from the diagonal matrix **S** gave the two most important of the orthonormal basis vectors that describe the 16 input spectra. The first row of $\mathbf{V^t}$, where t denotes a transpose, provided the fractions of each of the original spectra that composed the first basis vector. These fractions were used directly or in nearest-neighbor equations to estimate the relative contributions of individual nearest-neighbors or combinations of nearest-neighbors to the first basis vector. RMS deviations were calculated as $[(\sum(\text{spectrum1} - \text{spectrum2})^2/n]^{0.5}$, where the sum was over *n* wavelengths.

Calculations of Melting Temperatures for Unmodified Hybrids. Melting temperatures for analogous unmodified DNA·RNA hybrid sequences, but 12 base pairs in length, were calculated using thermodynamic data from Sugimoto et al. (1995) for two-state transitions of hybrid oligomers in a buffer containing 1 M NaCl (1 M NaCl, 10 mM Na_2HPO_4, 1 mM Na_2EDTA, pH 7.0). $\Delta H°$ and $\Delta S°$ were first calculated for each sequence, using nearest-neighbor values for the thermodynamic parameters of a set of 20 independent nearest-neighbor combinations (Gray, 1997). T_m values were then calculated at 100 μM total strand concentration using the formula $T_m(°C) = \Delta H°/(\Delta S° + R \ln(\text{conc})/4)) - 273.2$ for a two-state transition of non-self-complementary strands (Marky & Breslauer, 1987). For T_m values in Table 4, the sequences were taken to be 12 base pairs in length since this was the maximum length of the hybrid duplexes in the original data set. Similarly calculated T_m values fitted the reported T_m values (at 100 μM strand concentration) of the 64 oligomers from which the thermodynamic values were derived with a standard deviation of 1.6 °C.

RESULTS

Formation of S-DNA·RNA Hybrid Duplexes. It was possible to form hybrid duplexes from a wide range of simple, repeating sequences. These included the four possible repeating dinucleotide sequences (nos. 5−8 in Table 1) that did not involve the self-complementary single-stranded sequences S-d(AT) or S-d(GC). Among the eight possible repeating trinucleotide sequences that contain three different types of base pairs, six were tried (nos. 1, 3, 4, 13, 14, and 16) and five of them formed without difficulty. The S-d$(ACG)_8$ + r$(CGU)_8$ pair required heating to disrupt intrastrand complexes. There are four repeating trinucleotide sequences that have all purines or all pyrimidines on the same strand. The two with pyrimidines on the S-DNA strand (nos. 2 and 15) formed duplexes, although the S-d$(CCT)_8$ + r$(AGG)_8$ pair also had to be heated to overcome intrastrand pairing. We did not succeed in forming duplexes of repeating trinucleotides when there were all purines on the S-DNA strand; the S-d$(AAG)_8$ and r$(CUU)_8$ pair preferred to form a triplex, and the S-d$(AGG)_8$ sequence formed a stable self-complex, presumably due to aggregation of G's. Therefore, tetranucleotide sequences (nos. 9−12 in Table 1) were used to make hybrids having the S-d(AA)·r(UU) and S-d(GG)·r(CC) nearest-neighbor base pairs.

CD measurements provided an excellent means of monitoring the formation of hybrids from the separate strands. Figure 1 illustrates the significant CD changes that generally occurred during formation of the S-DNA·RNA hybrid duplexes. This figure shows the CD spectra of mixtures of S-d$(AGT)_8$ and r$(ACU)_8$ containing different mole percentages of each strand. The spectra of mixtures containing single-stranded S-d$(AGT)_8$ and up to 50% r$(ACU)_8$ had an isodichroic point at 244−245 nm (Figure 1A), and spectra of mixtures containing single-stranded r$(ACU)_8$ and up to 50% S-d$(AGT)_8$ had different isodichroic points at 263 and 225 nm (Figure 1B). That is, the spectra fell into two families with a breakpoint at 50 mol % of each of the oligomers. The CD spectrum of the hybrid duplex [the 50:50 mixture of S-d$(AGT)_8$ and r$(ACU)_8$] was significantly different from the spectra of the individual single strands or their average (not shown). Compared with the average spectrum, the duplex had a larger positive long-wavelength band, a new negative band at 210 nm, and a crossover that was shifted to shorter wavelengths by about 10 nm.

CD and OD mixing curves provided a further check as to whether each pair of oligomers formed a duplex when mixed in a 1:1 stoichiometry. Example mixing curves are shown in Supporting Information Figure 1 for repeat mixtures of S-d$(AGT)_8$ and r$(ACU)_8$. Breakpoints close to the expected 1:1 molar strand ratio were found for the 14 pairs listed in Table 1 that did not require heating. This also meant that the extinction coefficients for unmodified DNAs were adequate for the determination of S-DNA strand concentra-

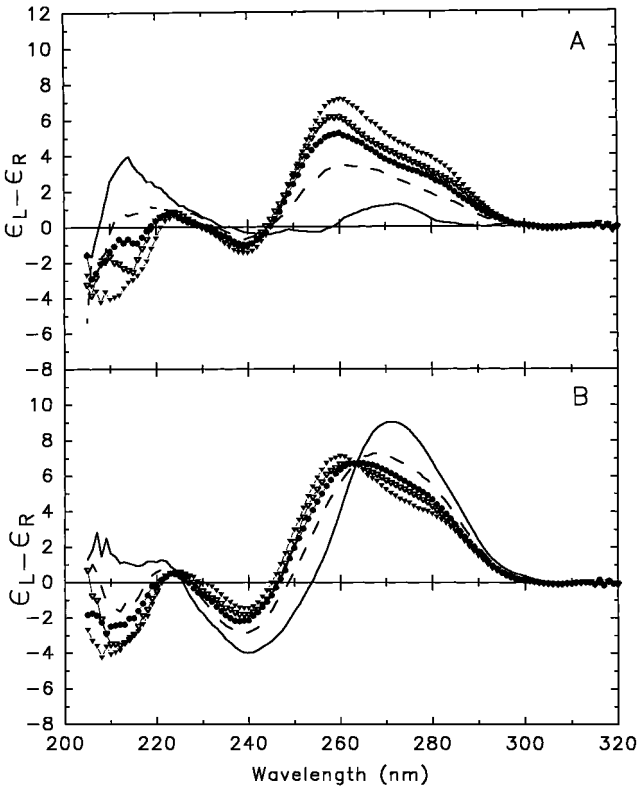

FIGURE 1: CD Spectra of mixtures of S-d$(AGT)_8$ + r$(ACU)_8$. (A) Samples containing 100−50% of S-d$(AGT)_8$. (B) Samples containing 100−50% r$(ACU)_8$. For the respective panels, 100% (—), 80% (- - - -), 67% (●), 60% (▽), 50% (▼) S-d$(AGT)_8$ or r$(ACU)_8$. Except as noted, the data in this and the following figures were taken with samples at 20 °C in 0.15 M K^+(phosphate), pH 7.

tions. The CD spectra of mixtures of the other two pairs, especially in the appearance of bands at 210 nm, were consistent with duplex formation.

CD Characteristics of S-DNA·RNA Hybrid Structures. The averaged CD spectra of the 16 hybrid duplexes are shown in Figure 2, and difference CD spectra, obtained by subtracting the spectra of the component single strands from the spectra of the duplexes, are shown in Supporting Information Figure 2. Panel A contains spectra of hybrids with 67% A + T(U), panels B and C contain spectra of repeating dinucleotide and tetranucleotide hybrids with 50% A + T(U), and panel D has spectra of the hybrids with 33% A + T(U). The spectra of the duplexes overall exhibited sequence-dependent characteristics, such as the breadth and composition of the positive bands above 240 nm, that to some extent were intermediate between the spectral features of the DNA B and RNA A forms. However, the duplexes also had common features of a composite positive band above about 250 nm, a negative band at 210 nm, and often a negative band at 230−250 nm.

The spectra of repeating dinucleotide sequences in Figure 2B clearly show that reversing the base sequences between the strands can markedly affect the CD spectrum [i.e. compare spectra of S-d$(AG)_{12}$·r$(CU)_{12}$, ○, and S-d$(CT)_{12}$·r$(AG)_{12}$, □, and spectra of S-d$(GT)_{12}$·r$(AC)_{12}$, ●, and S-d$(AC)_{12}$·r$(GU)_{12}$, ▽]. There are also sets of sequences in Figure 2A [S-d$(AGT)_8$·r$(ACU)_8$, ○, and S-d$(ACT)_8$·r$(AGU)_8$, □] and 4D [S-d$(AGC)_8$·r$(GCU)_8$, ○, and S-d$(GCT)_8$·r$(AGC)_8$, ●] that show the effects of reversing the sequences in the DNA and RNA strands. These differences are not just related to hybrids with r(purine)·d(pyrimidine and d(purine)·r(pyrimidine) strands.

The presence of U *versus* T chromophores in the same structure could be responsible for differences of 2−4 ($\epsilon_L - \epsilon_R$) centered at 270−280 nm, from our previous work on hybrids and dsDNA (Gray & Ratliff, 1975; Steely et al., 1986). Such differences caused by U *versus* T chromophores may enhance differences in CD contributions of the 16 possible nearest-neighbor base pairs but would not explain the wide range of CD changes observed upon reversing base sequences between the strands. A more adequate explanation is probably that DNA·RNA hybrids have a heteronomous conformation in solution (see Introduction) and that the CD spectrum reflects the differences in interactions of the same nearest-neighbor base pairs when they are reoriented on chemically different strands. There could also be spectral effects due to sequence-dependent variations in conformation.

CD spectra of the five homopurine·homopyrimidine sequences, S-d$(CTT)_8$·r$(AAG)_8$, S-d$(CT)_{12}$·r$(AG)_{12}$, S-d$(CCT)_8$·r$(AGG)_8$, S-d$(AAGG)_8$·r$(CCUU)_8$, and S-d$(AG)_{12}$·r$(CU)_{12}$, could be compared with published CD spectra of the analogous hybrid oligomers (24 base pairs long, in 0.05 M Na^+) containing normal DNA (Hung et al., 1994). The long wavelength positive bands were among the largest for the S-d(pur)·r(pyr) sequences and among the smallest for the S-d(pyr)·r(pur) sequences, and a relatively large 210 nm band was present for two of the three S-d(pyr)·r(pur) sequences, all in agreement with spectra for normal hybrid sequences. The only exception was S-d$(CCT)_8$·r$(AGG)_8$, in that it had one of the smallest 210 nm bands (Figure 2D, ▽). This sequence had to be heated to form a duplex, as noted above, and also had the largest δT_m (see below). While these characteristics suggested that samples of this sequence may not have consisted of uniformly formed duplexes, the melting temperatures of eight samples of S-d$(CCT)_8$·r$(AGG)_8$ were the highest of all the sequences measured (66.6 °C) and were quite reproducible (± 0.5 °C). The CD spectrum and T_m of this sequence were therefore cautiously included as being representative of the duplex.

The CD spectra of S-d$(AC)_{12}$·r$(GU)_{12}$ and S-d$(GT)_{12}$·r$(AC)_{12}$ above 220 nm closely matched those for the unmodified hybrid polymers of the same base sequences in 0.02 M Na^+ (Gray & Ratliff, 1975). This indicated that spectral effects of the oligomer ends were minimal. The absence of an effect of phosphorothioate substitution on the conformations of these hybrid sequences has also been found by Clark et al., 1997. In total, the CD spectra of the modified hybrids were remarkably unaffected by the phosphorothioate substitution.

The difference spectra (Supporting Information Figure 2) also showed significant variation with sequence. A dominant feature evident in the difference spectra was a negative difference band at or near 210 nm, demonstrating that this band arose from base pairing and stacking during the formation of the hybrid duplexes.

Singular Value Decomposition. Singular value decompositions of the hybrid duplex and difference spectra yielded the most significant spectral components of the respective duplex and difference spectra. There were at most seven significant basis vector components to each set of spectra. The two most significant components for each, the hybrid

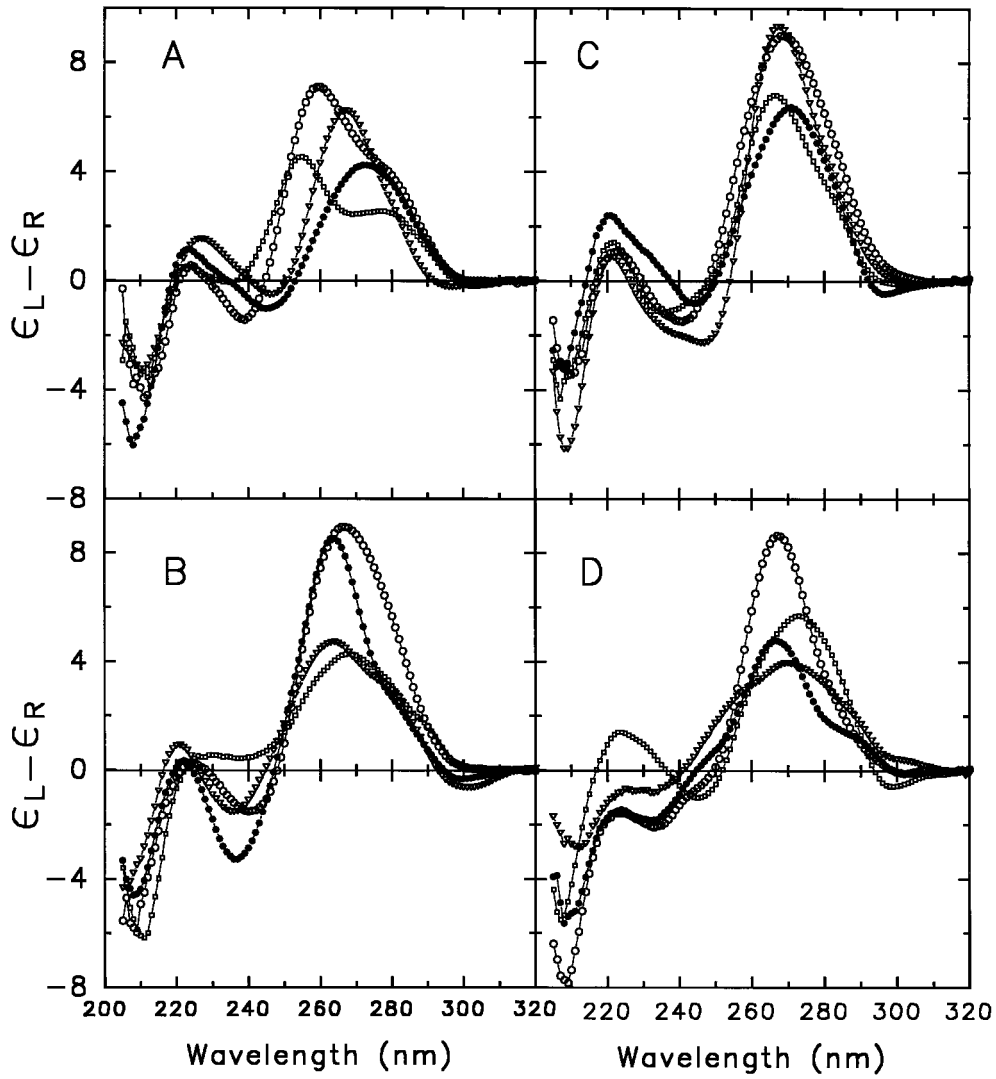

FIGURE 2: CD spectra of 16 hybrids formed from the 16 pairs of S-DNA and RNA oligomers listed in Table 1. (A) Hybrids from oligomer pairs containing 67% A + T(U): S-d$(AGT)_8$ + r$(ACU)_8$ (○), S-d$(CTT)_8$ + r$(AAG)_8$ (●), S-d$(ATC)_8$ + r$(GAU)_8$ (▽), and S-d$(ACT)_8$ + r$(AGU)_8$ (□). (B) Hybrids formed from repeating dinucleotide oligomer pairs containing 50% A + T(U): S-d$(AG)_{12}$ + r$(CU)_{12}$ (○), S-d$(GT)_{12}$ + r$(AC)_{12}$ (●), S-d$(AC)_{12}$ + r$(GU)_{12}$ (▽), and S-d$(CT)_{12}$ + r$(AG)_{12}$ (□). (C) Hybrids formed from repeating tetranucleotide oligomer pairs containing 50% A + T(U): S-d$(AAGG)_6$ + r$(CCUU)_6$ (○), d$(AACG)_6$ + r$(CGUU)_6$ (●), d$(AAGC)_6$ + r$(GCUU)_6$ (▽), and d$(AACC)_6$ + r$(GGUU)_6$ (□). (D) Hybrids formed from oligomer pairs containing 33% A + T(U): S-d$(AGC)_8$ + r$(GCU)_8$ (○), S-d$(GCT)_8$ + r$(AGC)_8$ (●), S-d$(CCT)_8$ + r$(AGG)_8$ (▽), and S-d$(ACG)_8$ + r$(CGU)_8$ (□). Each spectrum is the average of 3−4 determinations.

duplex and difference spectra, are shown in Figure 3. The major basis vector component of the duplex spectra is like that of A-RNA, in having a large, broad positive band above 250 nm and a negative 209−210 nm band (Gray et al., 1981). The 209−210 nm bands of the first basis vectors from the hybrid duplex and difference spectra were almost identical. Therefore, this negative band is mainly a consequence of forming the hybrid duplexes from the single strands. The positive band at about 268 nm of the first basis vector for the duplex spectra is only partially caused by changes during duplex formation; it also has a significant contribution from the inherent CD spectra of the component single-strands.

Nearest-Neighbor Calculations. As explained in Materials and Methods, the relative contributions of the original sequences to the major basis vector for the duplexes could be derived from information in the **V** matrix. These could be further divided into contributions assigned to combinations of the different nearest-neighbors. The contributions of repeating dinucleotide hybrid sequences (i.e. nos. 5−8 in Table 1) were assumed to be the average of the two types of constituent dinucleotide neighbors. The average contributions of S-d(AT)/r(AU) + S-d(TA)/r(UA) and of S-d(GC)/r(GC) + S-d(CG)/r(CG), and contributions for the four individual "like" neighbors S-d(AA)/r(UU), S-d(GG)/r(CC), etc., were estimated by nearest-neighbor combinations of the values for the other sequences, assuming that end effects could be neglected and the contributions of given nearest-neighbors were the same in all the sequences. Nearest-neighbor equations could be written that were correct to within 1−1.5 out of 23 internal nearest-neighbors. (There are 23 neighboring base pairs in oligomers 24 base pairs long.) For example, for a property, P, such as the contribution to the first hybrid basis vector:

$$\mathrm{P[S\text{-}d(AT)/r(AU) + S\text{-}d(TA)/r(UA)]} = \{3\mathrm{P[S\text{-}d(ATC)_8{\cdot}r(GAU)_8]} + 3\mathrm{P[S\text{-}d(ACT)_8{\cdot}r(AGU)_8]} - 2\mathrm{P[S\text{-}d(AC)_{12}{\cdot}r(GU)_{12}]} - 2\mathrm{P[S\text{-}d(CT)_8{\cdot}r(AG)_8]}\}/2$$

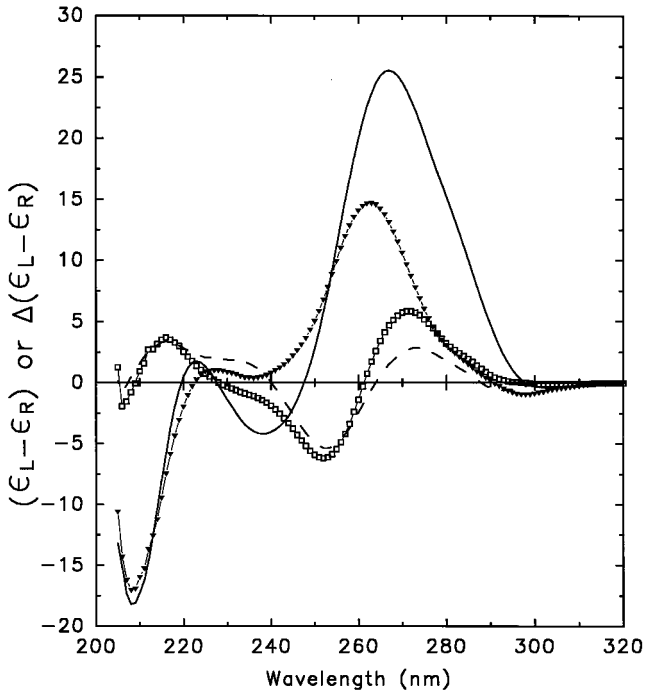

FIGURE 3: Most significant (—) and second most significant (- - - -) basis vector components from the singular value decomposition of the spectra of 16 hybrids in Figure 2. Most significant (▼) and second most significant (□) basis vector components from the singular value decomposition of 16 difference spectra in Figure 2 in Supporting Information.

Two equally accurate calculations for the S-d(AA)/r(UU) nearest-neighbor were possible, and the values from these were averaged:

$$P[\text{S-d(AA)/r(UU)}] = 4P[\text{S-d(AACG)}_6\cdot\text{r(CGUU)}_6] - 3P[\text{S-d(ACG)}_8\cdot\text{r(CGU)}_8],$$

and

$$P[\text{S-d(AA)/r(UU)}] = 4P[\text{S-d(AAGC)}_6\cdot\text{r(GCUU)}_6] - 3P[\text{S-d(AGC)}_8\cdot\text{r(GCU)}_8].$$

The 10 simplest combinations of the 16 nearest-neighbors are shown in Table 2. It was thus possible to distinguish contributions of the nearest-neighbor base pairs having the bases on different strands, for example S-d(GG)/r(CC) and S-d(CC)/r(GG), etc. The relative contributions of these to the major basis spectrum of the hybrids shown in Figure 3 are given in Table 2. Another index is the measured CD magnitude at a given wavelength, and the relative contributions to the CD at 267 nm are also listed. The range of values for the two calculations for S-d(AA)/r(UU)] gives an assessment of the uncertainty using the nearest-neighbor assumption and equations in which the nearest-neighbors are not balanced by 4−6%. For both columns of values in Table 2, the four nearest-neighbor combinations that contribute most are the same. While these four rows include the d(purine)·r(pyrimidine) nearest-neighbors, they also include an alternating purine−pyrimidine sequence. Moreover, there is a continuum of values that includes all the nearest-neighbors. Thus, the differences seen visually in the spectra of strand isomers in Figure 2 can be described in terms of different nearest-neighbor assignments once it is realized that the hybrid nearest-neighbor base pairs may each have a different CD contribution in a heteronomous structure.

Table 2: Nearest-Neighbors That Contribute to the Major CD Basis Vector Component of S-DNA·RNA Hybrids and to the CD at 267 nm

		relative contribution to:	
	nearest-neighbor or combination[a]	1st hybrid basis vector	CD at 267 nm
1	S-d(GG)/r(CC)	1.00	0.88
2	[S-d(AG)/r(CU) + S-d(GA)/r(UC)]/2	0.87	0.89
3	[S-d(GT)/r(AC) + S-d(TG)/r(CA)]/2	0.70	0.78
4	S-d(AA)/r(UU)	0.67 ± 0.14[b]	1.00 ± 0.13[b]
5	[S-d(GC)/r(GC) + S-d(CG)/r(CG)]/2	0.66	0.70
6	[S-d(CT)/r(AG) + S-d(TC)/r(GA)]/2	0.50	0.42
7	[S-d(AC)/r(GU) + S-d(CA)/r(UG)]/2	0.48	0.45
8	S-d(TT)/r(AA)	0.35	0.26
9	[S-d(AT)/r(AU) + S-d(TA)/r(UA)]/2	0.34	0.43
10	S-d(CC)/r(GG)	0.26	0.30

[a] Values are for the four measured repeating dinucleotide sequences in Table 1 and for combinations of the measured sequences with the assumption that ends can be neglected. The value for S-d(AA)/r(UU) is the average of two calculations (involving S-d(AACG)$_6$·r(CGUU)$_6$ and S-d(AAGC)$_6$·r(GCUU)$_6$) that were equally exact in their nearest-neighbor combinations. [b] Average and range of two calculated values.

A test of how consistent the CD spectra of the hybrids are was to calculate the CD spectrum of one of the sequences from the combined CD spectra of other sequences by a nearest-neighbor formula. Such a calculation will result in a spectrum close to the measured spectrum if (a) the CD spectrum is indeed a nearest-neighbor property, (b) given nearest-neighbors make the same CD contribution to all the sequences whose spectra are being compared, and (c) the equations are closely balanced with respect to the nearest-neighbor compositions of the sequences being compared. Requirement b is met if the sequences all have the same structures. The sequence of S-d(AAGC)$_6$·r(GCUU)$_6$ was chosen to be the dependent sequence because its nearest-neighbor composition (from an SVD analysis) was the most represented among the remainder of the sequences. From the available sequences, three combinations were possible that provided the same composition of 23 internal nearest-neighbors as this dependent sequence, to within one-half of one nearest-neighbor. These combinations involved relating the spectrum of the dependent sequence to spectra of 11 of the remaining sequences and are (per mole base-pair):

$$4CD[\text{S-d(AAGC)}_6\cdot\text{r(GCUU)}_6] =$$

Calculation 1

$$= 2CD[\text{S-d(CT)}_{12}\cdot\text{r(AG)}_{12}] + 3CD[\text{S-d(AGT)}_8\cdot\text{r-(ACU)}_8] + 3CD[\text{S-d(GCT)}_8\cdot\text{r(AGC)}_8] + 4CD[\text{S-d-(AACC)}_6\cdot\text{r(GGUU)}_6] - 2CD[\text{S-d(GT)}_{12}\cdot\text{r(AC)}_{12}] - 3CD[\text{S-d(ACT)}_8\cdot\text{r(AGU)}_8] - 3CD[\text{S-d(CCT)}_8\cdot\text{r-(AGG)}_8] \quad (1)$$

Calculation 2

$$= 2CD[\text{S-d(CT)}_{12}\cdot\text{r(AG)}_{12}] + 3CD[\text{S-d(AGC)}_8\cdot\text{r-(GCU)}_8] + 4CD[\text{S-d(AACC)}_6\cdot\text{r(GGUU)}_6] - 2CD[\text{S-d-(AC)}_{12}\cdot\text{r(GU)}_{12}] - 3CD[\text{S-d(CCT)}_8\cdot\text{r(AGG)}_8] \quad (2)$$

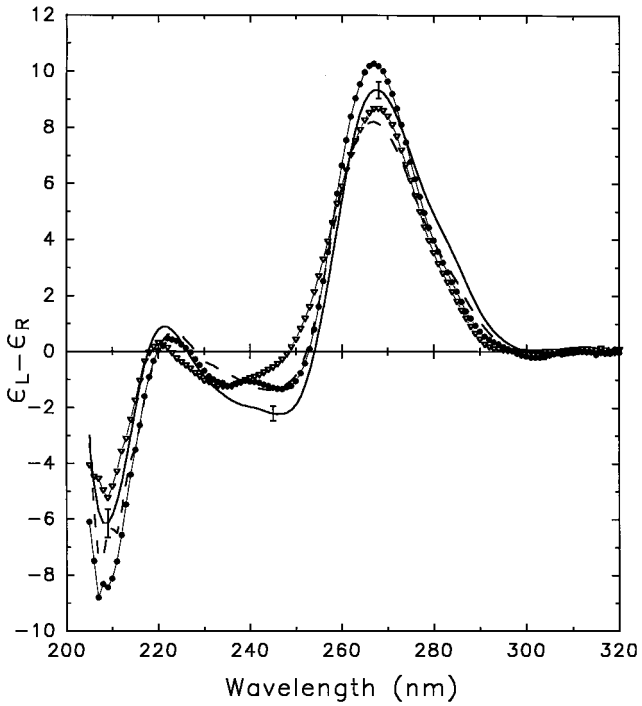

FIGURE 4: Measured *versus* calculated CD spectra for S-d(AAGC)$_6$·r(GCUU)$_6$. Average of four measured spectra (—) and spectra from nearest neighbor eqs 1 (- - - -), 2 (●), and 3 (▽) in the text. Error bars are the standard deviations of four measured spectra.

Calculation 3

$$= 3\text{CD}[\text{S-d(AGC)}_8\cdot\text{r(GCU)}_8] + 4\text{CD}[\text{S-d(AACG)}_6\cdot\text{r-(GGUU)}_6] - 3\text{CD}[\text{S-d(ACG)}_8\cdot\text{r(CGU)}_8] \quad (3)$$

The results of these calculations are plotted in Figure 4 along with the measured spectrum of S-d(AAGC)$_6$·r(GCUU)$_6$. Each calculation matches the measured S-d(AAGC)$_6$·r(GCUU)$_6$ spectrum well in general shape. Although they do not fit the measured spectrum to within the measurement error, shown by error bars at the band peaks of the measured spectrum, they do fit as well as do nearest-neighbor calculations of the CD spectra of dsRNA polymers (Gray et al., 1981). Four nearest-neighbor calculations of dsRNA spectra in the previous work had RMS deviations ranging from 0.63 to 1.05 M^{-1} cm^{-1}, while those in Figure 4 had RMS deviations of 0.76 to 0.99 M^{-1} cm^{-1}, over essentially the same wavelength range used in the previous work. Double-stranded RNAs are restricted to A or A′ conformations with C3′-endo sugars (Saenger, 1984). Since CD spectra of 12 of the hybrid sequences are related by the above formulas, the sequence-dependence of at least these 12 of the CD spectra shown in Figure 2 are consistent with the notion that the hybrids are also all in a similar conformation, but with the different nearest-neighbors having unique CD contributions. The other four hybrids (formed from pairs nos. 2, 3, 5, and 9 of Table 1) have independent sequences, and their CD spectra cannot be interrelated with the others that are available by nearest-neighbor formulas.

Melting Profiles and Melting Temperatures. An example melting profile for S-d(AAGC)$_6$·r(GCUU)$_6$ and its first derivative are plotted in Figure 5. Percent hyperchromicities, %H [given as the total percent increase in OD(260) between 20 and 90 °C or as the percent increase over the cooperative portion of the transition], and δT_m values (the temperature range over which 80% of the cooperative portion of the transition took place) are listed in Table 3 for all the sequences. The total %H values were in the range of 18.7 to 36.5%, and the δT_m values generally fell within a range

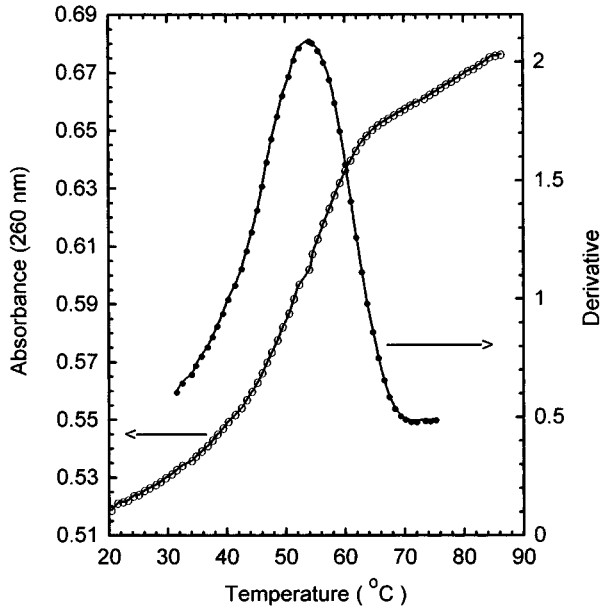

FIGURE 5: Example melting profile for the S-d(AAGC)$_6$·r(GCUU)$_6$ hybrid duplex. Absorbance at 260 nm (○), first derivative (●).

Table 3: Percent Hyperchromicities and Breadth of Melting Transitions for 16 S-DNA·RNA Hybrids in 0.15 M K^+ (phosphate buffer, pH 7.0), Except As Noted

sequence	total H%[a]	transition H%[b]	δT_m °C[c]
	67% A + T(U)		
S-d(ACT)$_8$·r(AGU)$_8$	32.4 ± 1.1[d]	24.4 ± 1.3[d]	19.4 ± 1.2[d]
S-d(ACT)$_8$·r(AGU)$_8$[e]	30.6 ± 2.2	22.8 ± 2.3	18.4 ± 0.5
S-d(ACT)$_8$·r(AGU)$_8$[e,f]	30.4	21.8	17.9
S-d(AGT)$_8$·r(ACU)$_8$	36.5 ± 1.4	27.1 ± 0.9	14.8 ± 0.5
S-d(ATC)$_8$·r(GAU)$_8$	33.2 ± 1.7	23.3 ± 1.6	17.7 ± 0.7
S-d(ATC)$_8$·r(GAU)$_8$[e]	31.7 ± 1.4	23.8 ± 0.9	17.8 ± 0.5
S-d(ATC)$_8$·r(GAU)$_8$[e,f]	32.2	23.5	18.2
S-d(CTT)$_8$·r(AAG)$_8$	23.3 ± 4.4	16.4 ± 2.4	23.6 ± 1.7
	50% A + T(U)		
S-d(AAGG)$_6$·r(CCUU)$_6$	26.3 ± 0.4	18.6 ± 1.1	20.7 ± 2.0
S-d(AG)$_{12}$·r(CU)$_{12}$	33.7 ± 2.5	24.9 ± 1.7	20.1 ± 1.3
S-d(AG)$_{12}$·r(CU)$_{12}$[f]	31.7 ± 0.7	24.4 ± 1.2	19.7 ± 1.2
S-d(AACG)$_6$·r(CGUU)$_6$	27.5 ± 1.4	19.8 ± 0.8	21.0 ± 0.7
S-d(AACC)$_6$·r(GGUU)$_6$	24.1 ± 1.2	17.7 ± 0.6	19.7 ± 1.0
S-d(AAGC)$_6$·r(GCUU)$_6$	31.2 ± 1.9	22.4 ± 1.3	21.0 ± 0.6
S-d(AC)$_{12}$·r(GU)$_{12}$	26.4 ± 1.7	19.6 ± 1.3	20.0 ± 0.8
S-d(CT)$_{12}$·r(AG)$_{12}$	24.4 ± 5.0	16.3 ± 3.3	23.0 ± 1.4
S-d(GT)$_{12}$·r(AC)$_{12}$	31.4 ± 2.2	24.0 ± 2.0	18.4 ± 1.1
S-d(GT)$_{12}$·r(AC)$_{12}$[f]	28.7 ± 1.1	21.9 ± 0.2	17.8 ± 0.3
	33% A + T(U)		
S-d(ACG)$_8$·r(CGU)$_8$	28.1 ± 1.3	21.2 ± 1.2	21.0 ± 0.6
S-d(AGC)$_8$·r(GCU)$_8$	27.6 ± 1.6	20.8 ± 0.8	19.1 ± 1.1
S-d(GCT)$_8$·r(AGC)$_8$	26.1 ± 4.0	18.2 ± 2.9	20.8 ± 1.0
S-d(CCT)$_8$·r(AGG)$_8$	18.7 ± 1.4	15.8 ± 1.5	30.0 ± 2.6

[a] The percent increase in OD_{260} between 20 and 90 °C. [b] The percent increase in OD_{260} over the cooperative portion of the transition that excluded upper and lower sloping baselines. [c] The temperature range over which 80% of the cooperative portion of the transition took place. [d] The standard deviations are from 6−8 melting profiles for each hybrid duplex in a buffer of 0.15 M K^+ (phosphate buffer, pH 7.0), except as noted. [e] 0.15 M Na^+ (phosphate buffer, pH 7.0); standard deviations, where given, are from 3 or 4 melting profiles. [f] Na^+ or K^+ (phosphate buffer, pH 7.0), plus 2 mM $MgCl_2$; the range of values, where given, is from duplicate melting profiles.

Table 4: Measured T_m Values for 16 S-DNA·RNA Hybrids in 0.15 M K^+ or with Other Ions, and Calculated T_m values for Normal DNA·RNA Hybrids in 1.0 M Na^+

	measured T_m (°C) S-DNA·RNA			calcd T_m (°C) DNA·RNA[f]
hybrid sequence	0.15 M K^+	other ions	1 M cation[e]	1 M Na^+
67% A + T(U)				
S-d$(ACT)_8$·r$(AGU)_8$	44.1 ± 0.2[a]	(43.2 ± 0.8)[b] [45.5 ± 0.5][c]		52.4
S-d$(AGT)_8$·r$(ACU)_8$	45.9 ± 0.1			53.9
S-d$(ATC)_8$·r$(GAU)_8$	46.9 ± 0.1	(46.5 ± 0.7)[b] [47.8 ± 0.4][c]	57.0 ± 0.5	54.5
S-d$(CTT)_8$·r$(AAG)_8$	48.7 ± 1.4			60.2
50% A + T(U)				
S-d$(AAGG)_6$·r$(CCUU)_6$	44.2 ± 1.1			52.9
S-d$(AG)_{12}$·r$(CU)_{12}$	46.4 ± 0.6	{47.5 ± 0.1}[d]	60.0 ± 0.9	53.4
S-d$(AACG)_6$·r$(CGUU)_6$	46.5 ± 0.4		55.4 ± 0.1	49.1
S-d$(AACC)_6$·r$(GGUU)_6$	52.2 ± 1.1			59.4
S-d$(AAGC)_6$·r$(GCUU)_6$	54.2 ± 0.4		65.8 ± 1.1	59.3
S-d$(AC)_{12}$·r$(GU)_{12}$	54.4 ± 0.3		64.4 ± 0.6	55.9
S-d$(CT)_{12}$·r$(AG)_{12}$	57.4 ± 1.5			70.1
S-d$(GT)_{12}$·r$(AC)_{12}$	57.6 ± 0.4	{57.8 ± 0.6}[d]		63.7
33% A + T(U)				
S-d$(ACG)_8$·r$(CGU)_8$	56.7 ± 0.5			59.0
S-d$(AGC)_8$·r$(GCU)_8$	63.0 ± 0.7			77.1
S-d$(GCT)_8$·r$(AGC)_8$	64.9 ± 0.7			75.9
S-d$(CCT)_8$·r$(AGG)_8$	66.6 ± 0.5			81.7

[a] The standard deviations are from 6−8 melting profiles for each hybrid duplex in a buffer of 0.15 M K^+ (phosphate buffer, pH 7.0). [b] T_m values in 0.15 M Na^+ (phosphate buffer, pH 7.0); standard deviations from 3−4 melting profiles. [c] T_m values in 2 mM $MgCl_2$ plus 0.15 M Na^+ (phosphate buffer, pH 7.0); standard deviations from three melting profiles. [d] T_m values in 2 mM $MgCl_2$ + 0.15 M K^+ (phosphate buffer, pH 7.0); the range of values from duplicate melting profiles. [e] T_m values in 0.90 M Na^+ plus 0.11 M K^+; standard deviations from three melting profiles. [f] Calculated from data in Sugimoto et al. (1995) for hybrids 12 base pairs long at 100 μM total strand concentration (in 1M NaCl, 1 mM Na_2HPO_4, and 1 mM Na_2EDTA, pH 7.0); standard deviation is 1.6 °C from similarly calculated values compared with published T_m data for the same concentration; see Materials and Methods.

of 17.7 to 23.6 °C. These values were respectively greater and less in magnitude than previously found for hybrids 24 nucleotides long that did not contain phosphorothioated DNA (in 0.05 M Na^+, Hung et al., 1994). The only melting profile with a δT_m (30 °C) outside of the above range was that for S-d$(CCT)_8$·r$(AGG)_8$. All of the hybrid duplexes had significant hyperchromicities at 260 nm and exhibited cooperative melting profiles, generally with δT_m values of less than 24 °C. This indicated that the samples essentially consisted of fully formed duplexes and that melting transitions were not obviously broadened by the existence of a random mixture of *R* and *S* conformers. The melting profile in Figure 5 was one of the broader profiles with a δT_m of 21 °C.

The CD and absorbance changes upon melting were reversible upon cooling at room temperature (not shown), as was routinely checked after each melting experiment. The CD spectra of the melted hybrids at 90°C were also routinely compared with and were found to be essentially identical to the averaged spectra of the heated single strands.

Multiple melting profiles in 0.15 M K^+ (phosphate buffer, pH 7.0) were acquired for at least three independently formed samples of each S-DNA·RNA hybrid. The melting temperatures, determined from the peaks of the derivatives, are listed in Table 4 for the 16 hybrid sequences in order of increasing T_m for oligomers of the same A + T(U) composition. The T_m values spanned a range of 22.5 °C, from 44.1 to 66.6 °C. Although the T_m values generally increased with increasing (G + C)-content, there was a considerable effect of the neighboring base pair content. For example, there was a 13.4 °C variation among the sequences having 50% A + T/(U), and the most stable and least stable of these sequences overlapped those having higher and lower (G + C)-contents, respectively. The sequence-dependence of the measured T_m values was consistent with the well-known importance of the strand asymmetry of purines and pyrimidines in unmodified hybrids, d(pur)·r(pyr) sequences being less stable than the analogous d(pyr)·r(pur) sequences (Roberts et al., 1992; Hung et al., 1994; Ratmeyer, et al., 1994; Lesnik & Freier 1995; Gyi et al., 1996). For example, S-d$(CTT)_8$·r$(AAG)_8$, S-d$(CT)_{12}$·r$(AG)_{12}$, and S-d$(CCT)_8$·r$(AGG)_8$ were among the most thermostable of sequences of the same A +T(U) content, while S-d$(AAGG)_8$·r$(CCUU)_8$ and S-d$(AG)_{12}$·r$(CU)_{12}$ were the least stable of the sequences of 50% A + T(U).

The melting temperatures measured for the 16 S-DNA·RNA oligomer hybrids had a sequence-dependence that was close to that calculated for normal DNA·RNA hybrids based on published two-state thermodynamic parameters for 64 oligomers of normal DNA·RNA hybrids 5−12 base pairs long in 1 M NaCl (Sugimoto et al., 1995), as described in Materials and Methods. T_m values were calculated for analogous unmodified sequences 12 base pairs in length at 100 μM strand concentration and are shown in the last column of Table 4. Calculated values were dependent on the length of the sequence, and sequences 12 base pairs were the longest for which the calculated values were taken to be reliable. Relative calculated values were not very dependent on concentration, generally varying no more than 3 °C in their relative values over the range of 2.5 to 400 μM in strand concentration. Exceptions were d$(AAGG)_3$·r$(CCUU)_3$ and d$(AG)_6$·r$(CU)_6$, whose calculated T_m values decreased about 4 °C more than average with decreasing concentration. The rather similar magnitudes of some of the measured and calculated values in the first and last columns of Table 4 are fortuitous given that solution conditions are different, that phosphorothioate-substitution reduces the T_m of S-DNA·

RNA hybrids, and that the measured melting transitions are for sequences 24 base pairs long and are not two-state. The purpose of the comparison is only to compare the sequence dependence of measured T_m values for S-DNA·RNA hybrid sequences with that calculated from available data for normal hybrid sequences, not to compare absolute melting temperatures. The ranking of the calculated melting temperatures for the analogous unmodified sequences was remarkably the same as the ranking of measured T_m values for S-DNA·RNA hybrids of the same G + C content, with a correlation coefficient of 0.93, with possible significant exceptions. The largest difference was for the sequences $d(CT)_6$·$r(AG)_6$ and $d(GT)_6$·$r(AC)_6$, which were similar in their measured T_m values but differed by more than 6 °C in their calculated values throughout the concentration range considered.

To test whether cation concentration might influence the relative measured T_m values, melting temperatures were measured for five of the S-DNA·RNA hybrids at 1 M cation concentration (0.90 M Na^+ plus 0.11 M K^+). Three of the five sequences chosen [S-$d(ATC)_8$·$r(GAU)_8$, S-$d(AG)_{12}$·$r(CU)_{12}$, and S-$d(AACG)_8$·$r(CGUU)_8$] had indistinguishable T_m values of 46.4 to 46.9 °C in 0.15 M K^+, while the calculated melting temperatures at 1 M Na^+ for normal DNA·RNA hybrids with these sequences varied by 5.4 °C, from 49.1 to 54.5 °C. Likewise, the other two sequences chosen [$d(AAGC)_8$·$r(GCUU)_8$ and S-$d(AC)_{12}$·$r(GU)_{12}$] had the same T_m of 54.2−54.4 °C at low salt concentration but there was a difference of 3.4 °C at 1 M Na^+ for normal hybrids of these sequences. Upon increasing the cation concentration to 1 M, the measured T_m values of the S-DNA·RNA hybrids all increased, by an average of 10.8 °C, but became slightly different so that they correlated even more closely with those calculated for the unmodified sequences.

Influence of Mg^{2+} Combined with Na^+ or K^+. The effects of different ions on the melting temperatures and CD spectra were surveyed. The melting temperatures of two sequences, S-$d(ACT)_8$·$r(AGU)_8$ and S-$d(ATC)_8$·$r(GAU)_8$, were determined in 0.15 M Na^+ (phosphate buffer, pH 7) and found to be lower than in 0.15 M K^+ (phosphate buffer, pH 7) by 0.9 and 0.4 °C, respectively. See Table 4. These differences were not significant, however, within the standard deviations of the measurements. The influence of 2 mM Mg^{2+} added to either the Na^+ buffer [for S-$d(ACT)_8$·$r(AGU)_8$ and S-$d(ATC)_8$·$r(GAU)_8$] or K^+ buffer [for S-$d(AG)_{12}$·$r(CU)_{12}$ and S-$d(GT)_{12}$·$r(AC)_{12}$] was to slightly increase the T_m by 2.3, 1.3, and 1.1 °C, respectively, for the first three of these sequences, but not to change the T_m of S-$d(GT)_{12}$·$r(AC)_{12}$, which had the highest T_m of the four sequences tested (Table 4). Since the intracellular concentration of free Mg^{2+} is less than 1 mM (Gupta & Yushok, 1980) and the cellular K^+ ion concentration is like that of our buffer, the *in vivo* melting temperatures of the S-DNA·RNA hybrid sequences could be close to those in Table 4 despite other complexities of the *in vivo* medium.

There were essentially no effects on the CD spectra of substituting Na^+ for K^+, or upon adding Mg^{2+} to either buffer. The spectra of the sequences with all six different Na^+, Na^+ plus Mg^{2+}, and K^+ plus Mg^{2+} ion combinations were measured and compared with the spectra of the sequences in 0.15 M K^+. These are shown in Supporting Information Figure 3. Since CD spectra are very sensitive to slight changes in nucleic acid conformation, we concluded that the hybrid duplex conformations were not affected by these different ion combinations.

DISCUSSION

CD Characteristics of S-DNA·RNA Hybrid Structures. Hybrid duplexes with simple, repeating sequences could be formed with phosphorothioated DNAs, allowing a wide range of sequence-dependent melting temperatures and CD spectral properties to be measured under physiological salt conditions. With two exceptions, all of the simple S-DNA sequences tested could be hybridized at room temperature. The spectra of seven of the sequences were found to be quite similar in characteristic details to published spectra of analogous hybrid sequences having unmodified DNA strands. The closeness of the comparisons above 220 nm indicated that the phosphorothioate strands did not affect the conformations of the hybrids, at least not the average conformation that is detected by CD measurements. End effects on the CD spectra also appeared to be minimal for these sequences that were 24 base pairs in length.

The dominant CD basis vector for the hybrid duplexes had features of CD spectra of natural RNAs, including a characteristic negative band near 210 nm, a broad positive band at 267 nm, and a small negative band at 238 nm (Gray et al., 1981). A band at 210 nm was a prominent feature induced by hybrid duplex formation. Another feature characteristic of most G·C-containing dsRNAs that was present in individual hybrid duplex spectra and in the second basis vector of the duplexes was a small negative CD band at 290−300 nm. Thus, the CD spectra of the S-DNA·RNA hybrids are dominated by the A conformation of the RNA strand plus the partial A-like character of the DNA strand.

There is ample evidence that DNA·RNA hybrids are heteronomous in conformation, with the DNA and RNA strands differing in structure, as reviewed in the Introduction. This means that the number of different nearest-neighbor base pairs is greater for hybrids (i.e. 16) than for dsRNA or dsDNA (i.e. 10). For this reason it is essential to study a wider range of hybrid sequences than of dsRNA or dsDNA sequences to document the full sequence-dependent range of a given property.

The stability and CD spectra differ for sequences in which the DNA and RNA strands have different base compositions (Roberts & Crothers, 1992; Ratmeyer et al., 1994; Hung et al, 1994; Lesnik & Freier, 1995; Gyi et al., 1996). The dramatic CD differences in spectra of d(purine)·r(pyrimidine) and r(purine)·d(pyrimidine) sequences of hybrids with unmodified DNA strands has been interpreted in our previous work (Hung et al., 1994) and by others as indicating the existence of different classes of conformations. Indeed, work by Gyi et al. (1996) shows that the DNA differs in flexibility in these two classes of hybrids, and Lesnik & Freier (1995) found that the electrophoretic mobility of hybrids was closer to that of dsRNA as the purine content of the RNA strand increased. However, our present CD spectra of a wider range of hybrid sequences with S-DNA strands, which seem to be quite similar to spectra of hybrids with normal DNA strands, show spectral differences that are not unique to homopurine·homopyrimidine sequences (Figure 2 and Table 2). Twelve of the sequences have spectra that are related by nearest-

neighbor formulas at least as well as are spectra of dsRNA sequences (Figure 4 and Gray et al., 1981). A requirement for nearest-neighbor formulas to be valid is that each nearest-neighbor have the same value in all of the sequences being compared. Thus, the CD spectral differences for S-DNA·RNA hybrid sequences do not imply global differences in hybrid conformations that extend beyond the nearest-neighbors. A simpler model is that the CD spectra largely reflect very different chromophore interactions (including differences for T *versus* U) for each of the 16 possible nearest-neighbor base pairs in what could be a similar heteronomous conformation. Conformations of different types of nearest-neighbor base pairs could differ enough so as to affect other properties (e.g. electrophoretic mobility), but the conformation does not appear to vary dramatically among the occurrences of a given type of nearest-neighbor base pair in different sequences.

It is possible that there are global heteronomous conformations among our sequences that are not distinguished by our CD measurements. If there would be global conformational differences that result in different interactions of the same nearest-neighbor base pair in different sequences, the extraction of nearest-neighbor thermodynamic properties from hybrids would be more complex than has been assumed (Sugimoto et al., 1995). Fortunately, this does not appear to be the case, even for hybrids with phosphorothioate DNAs which have backbones that are a random mixture of *R* and *S* stereoisomers. Therefore, one important conclusion of our CD results is that hybrid conformations may not be so different as to require models of stability that extend beyond the nearest-neighbors. With respect to the use of S-DNAs in antisense therapy, there may be little reason to expect an enhanced RNAse H activity for hybrids formed from S-DNAs that are pyrimidine-rich relative to those that are purine-rich. Even though there may not be a major sequence-dependent conformational effect of S-DNA·RNA hybrids on recognition by RNase H, the sequences could differ in their ability to conform to and be cleaved in the RNAse H binding site.

Melting Temperatures. The sequence-dependence of melting temperatures for the modified S-DNA·RNA hybrids (in 0.15 M K^+) was similar to that calculated from the two-state thermodynamic parameters derived from unmodified DNA·RNA hybrids (in 1 M Na^+), despite the differences in conditions and the fact that our hybrids of 24 base pairs do not melt in a two-state fashion. The T_m values for five S-DNA·RNA hybrid sequences were studied at 1 M cation concentration to assess whether there were any contradictory sequence effects of the salt concentration. At 1 M cation concentration, the T_m values were all increased, but the rank of T_m values became slightly closer to that calculated for normal DNA·RNA hybrids. In general, the agreement of the measured and calculated melting temperatures, together with the agreement of CD spectra of modified and normal hybrids, indicated that the phosphorothioate modification does not selectively affect particular sequences in either conformation or thermal stability.

Measured T_m values of two hybrids were unchanged in 0.15 M Na^+, but the T_m values of three hybrids, those with the lowest T_m values of four tested, increased an average of 1.6 °C upon the addition of 2 mM Mg^{2+}.

In additional calculations, we found that the T_m values calculated for unmodified hybrids 12 base pairs long were not well correlated with values calculated for longer sequences from the same two-state data. Thus, it will be important for the predictions of melting temperatures to study the thermodynamic properties of hybrids formed with S-DNAs having a wide range of lengths, as well as at appropriate salt concentrations.

Although the T_m is not strictly a nearest-neighbor property, it has been previously observed that the T_m values of dsDNA and dsRNA polymers are approximately related as nearest-neighbor properties (Ratliff et al., 1973; Gray et al., 1981). Ornstein & Fresco (1983a,b) exploited these aproximate relationships among T_m values to calculate sets of apparent enthalpy values for dsDNA and dsRNA dinucleotide base pairs, and Vologodskii et al. (1984) used T_m values of natural dsDNAs to show that there are eight linearly independent sequence combinations of melting temperatures, as there should be for polymer nearest-neighbor properties (Gray & Tinoco, 1970). In the present work, we find that the T_m values in Table 4 are approximately related by the same nearest-neighbor formulas used above to calculate CD spectra for S-d$(AAGC)_6$·r$(GCUU)_6$. The calculated T_m values were 52.2, 51.0, and 51.2 °C, from eqs 1−3, respectively. These were the same to within 1.2 °C, and the values differed by only 2−3 °C from the measured T_m of 54.2 °C for S-d$(AAGC)_6$·r$(GCUU)_6$. The agreement seems significant, considering that the T_m values combined in eqs 1−3 span a range of 22.5 °C. Whatever its origin, this agreement among T_m values lends support to the view that the S-DNA·RNA hybrids do not fall into conformational classes in which nearest-neighbor properties are dramatically different.

ACKNOWLEDGMENT

We are grateful to Dr. R. L. Ratliff (Los Alamos National Laboratory) for synthesis of many of the oligomers, Mr. C. L. Clark (Program in Molecular and Cell Biology, University of Texas at Dallas) for programing the singular value decomposition routine, and Mr. D. Singh (Program in Molecular and Cell Biology, University of Texas at Dallas) for performing the gel electrophoresis analysis of the oligomers.

SUPPORTING INFORMATION AVAILABLE

Three figures in supporting material show (1) CD and OD mixing curves for repeat mixtures of the S-d$(AGT)_8$ + r$(ACU)_8$ pair whose CD spectra are plotted in text Figure 1, (2) difference CD spectra for all 16 hybrid sequences whose CD spectra are plotted in text Figure 2, and (3) CD spectra of sequences for the four S-DNA·RNA oligomer hybrids that were studied in the presence of K^+, Na^+, and/or Mg^{2+} ions, to illustrate the absence of specific ion effects (4 pages). Ordering information is given on any current masthead page.

REFERENCES

Agrawal, S., Mayrand, S. H., Zamecnik, P. C., & Pederson, T. (1990) *Proc. Natl. Acad. Sci. U.S.A. 87*, 1401−1405.

Allawi, H. T., & SantaLucia, J., Jr. (1997) *Biochemistry 36*, 10581−10594.

Arnott, S., Chandrasekaran, R., Milane, R. P., & Park, H.-S. (1986) *J. Mol. Biol. 188*, 631−640.
Baum, R. (1994) *Chem. Eng. News 72*, 21−22.
Benevides, J. M., Wang, A. H., Rich, A., Kyogoku, Y., van der Marel, G. A., van Boom, J. H., & Thomas, G. J., Jr. (1986) *Biochemistry 25*, 41−50.
Breslauer, K. J., Frank, R., Blöcker, H., & Marky, L. A. (1986) *Proc. Natl. Acad. Sci. U.S.A. 83*, 3746−3750.
Brown, D. A., Kang, S.-H., Gryaznov, S. M., DeDionisio, L., Heidenreich, O., Sullivan, S., Xu, X., & Nerenberg, M. I. (1994) *J. Biol. Chem. 269*, 26801−26805.
Callahan, D. E., Trapane, T. L., Miller, P. S., Ts'o, P. O. P., & Kan, L.-S. (1991) *Biochemistry 30*, 1650−1655.
Clark, C. L., Cecil, P. K., Singh, D., & Gray, D. M. (1997) *Nucl. Acids Res 25*, 4098−4105.
Cohen, J. S., & Hogan, M. E. (1994) *Sci. Am. 271*, 76−82.
Crooke, R. M., Graham, M. J., Cooke, M. E., & Crooke, S. T. (1995) *J. Pharmacol. Exp. Ther. 275*, 462−473.
Dean, N., McKay, R., Miraglia, L., Howard, R., Cooper, S., Giddings, J., Nicklin, P., Meister, L., Ziel, R., Geiger, T., Muller, M., & Fabbro, D. (1996) *Cancer Res. 56*, 3499−3507.
Ding, D., Gryaznov, S. M., Lloyd, D. H., Chandrasekaran, S., Yao, S., Ratmeyer, L., Pan, Y., & Wilson, W. D. (1996) *Nucl. Acids Res. 24*, 354−360.
Freier, S. M., Kierzek, R., Jaeger, J. A., Sugimoto, N., Caruthers, M. H., Neilson, T., & Turner, D. H. (1986) *Proc. Natl. Acad. Sci. 83*, 9373−9377.
González, C., Stec, W., Kobylanska, A., Hogrefe, R. I., Reynolds, M., & James, T. L. (1994) *Biochemistry 33*, 11062−11072.
González, C., Stec, W., Kobylanska, Reynolds, M., & James, T. L. (1995) *Biochemistry 34*, 4969−4982.
Gray, D. M. (1997) *Biopolymers*, in press.
Gray, D. M., Liu, J. J., Ratliff, R. L., & Allen, F. S. (1981) *Bioploymers 20*, 1337−1382.
Gray, D. M., Hung, S. H., & Johnson, K. H. (1995) *Methods Enzymol. 246*, 19−34.
Gray, D. M., & Tinoco, I., Jr. (1970) *Biopolymers 9*, 223−244.
Gray, D. M., & Ratliff, R. L., (1975) *Bioploymers 14*, 487−498.
Gray, G. D., Basu, S., & Wickstrom, E. (1997) *Biochem. Pharmacol. 53*, 1465−1476.
Gupta, R. K., & Yushok, W. D. (1980) *Proc. Natl. Acad. Sci. U.S.A. 77*, 2487−2491.
Gura, T. (1995) *Science 270*, 575−577.
Gutierrez, A. J., Matteucci, M. D., Grant, D., Matsumura, S., Wagner, R. W., & Froehler, B. C. (1997) *Biochemistry 36*, 743−748.
Gyi, J. I., Conn, G. L., Lane, A. N., & Brown, T. (1996) *Biochemistry 35*, 12538−12548.
Hall, K. B., & McLaughlin, L. W. (1991) *Biochemistry 30*, 10606−10613.
Henry, E. R., & Hofrichter, J. (1992) *Methods Enzymol. 210*, 129−192.
Hung, S.-H., Yu, Q., Gray, D. M., and Ratliff, R. L. (1994) *Nucl. Acids Res. 22*, 4326−4334.
Iversen, P. L., Zhu, S., Meyer, A., & Zon, G. (1992) *Antisense Res. Dev. 2*, 211−222.
Johnson, W. C, Jr. (1992) *Methods Enzymol. 210*, 426−447.
Johnson, W. C., Jr. (1994) in *Circular Dichroism Principles & Applications* (Nakaniski, K., Berova, N., & Woody, R. W., Eds.) pp 523−540, VCH Publishers, Inc., New York.
Khaled, Z., Benimetskaya, L., Zeltser, R., Khan, T., Sharima, H. W., Narayanan, R., & Stein, C. A. (1996) *Nucl. Acids Res. 24*, 737−745.
Lesnik, E. A., & Freier, S. M. (1995) *Biochemistry 34*, 10807−10815.
Lima, W. F., & Crooke, S. T. (1997) *Biochemistry 36*, 390−398.
Maltese, J. Y., Sharma, H. W., Vassilen, L., & Narayanan, R. (1995) *Nucl. Acids. Res. 23*, 1146−1151.
Marky, L. A., & Breslauer, K. J. (1987) *Biopolymers 26*, 1601−1620.
Matteucci, M. D, & Wagner, R. W. (1996) *Nature 384*, 20−22.
Monia, B. P., Lesnik, E. A., Gonzalez, C., Lima, W. F., McGee, D., Guinosso, C. J., Kawasaki, A. M., Cook, P. D., & Freier, S. M. (1993) *J. Biol. Chem. 268*, 14514−14522.
Nishizaki, T., Iwai, S., Ohkubo, T., Kojima, C., Nakamura, H., Kyogoku, Y., & Ohtsuka, E. (1996) *Biochemistry 35*, 4016−4025.
Oda, Y., Iwai, S., Ohtsuka, E., Ishikawa, M., Ikehara, M., & Nakamura, H. (1993) *Nucl. Acids Res. 21*, 4690−4695.
Ornstein, R. L., & Fresco, J. R. (1983a) *Biopolymers 22*, 1979−2000.
Ornstein, R. L., & Fresco, J. R. (1983b) *Biopolymers 22*, 2001−2016.
Perez, J. R., Li, Y., Stein, C. A., Majumder, S., Oorschat, A. V., & Narayanan, R. (1994) *Proc. Natl. Acad. Sci. U.S.A. 91*, 5957−5961.
Politz, J. C., Taneja, K. L., & Singer, R. H. (1995) *Nucl. Acids Res. 23*, 4946−4953.
Press, W. H., Teukolsky, S. A., Vetterling, W. T., & Flannery, B. P. (1992) *Numerical Recipes in C; The Art of Scientific Computing*, 2nd Ed., pp 59−70, Cambridge University Press, Cambridge, England.
Ratmeyer, L., Vinayak, R., Zhong, Y. Y., Zon, G., & Wilson, W. D. (1994) *Biochemistry 33*, 5298−5304.
Rice, J. S., & Gao, X. (1997) *Biochemistry 36*, 399−411.
Roberts, R. W., & Crothers, D. M. (1992) *Science 258*, 1463−1466.
Saenger, W. (1984) *Principles of Nucleic Acid Structure*, Springer-Verlag, New York, NY, pp 220−236.
Salazar, M., Fedoroff, O. Y., & Reid, B. R. (1996) *Biochemistry 35*, 8126−8135.
SantaLucia, J., Jr., Allawi, H. T., & Seneviratne, P. A. (1996) *Biochemistry 35*, 3555−3562.
Savitzky, A., & Golay, M. J. E. (1964) *Anal. Chem. 36*, 1627−1639.
Steely, H. T., Jr., Gray, D. M., & Ratliff, R. L. (1986) *Nucl. Acids Res. 14*, 10071−10090.
Stein, C. A. (1995) *Nat. Med. 1*, 1119−1121.
Stein, C. A., Subasinghe, C., Shinozuka, K., & Cohen, J. S. (1988) *Nucl. Acids Res. 16*, 3209−3221.
Stein, C. A., & Cheng, Y. C. (1993) *Science 261*, 1004−1012.
Stephenson, M. L., & Zamecnik, P. C. (1978) *Proc. Natl. Acad. Sci. U.S.A. 75*, 285−288.
Stull, R. A., Taylor, L. A., & Szoka, F. C., Jr. (1992) *Nucl. Acids Res. 20*, 3501−3508.
Sugimoto, N., Nakano, S., Katoh, M., Matsumura, A., Nakamuta, H., Ohmichi, T.,Yoneyama, M., & Sasaki, M. (1995) *Biochemistry 34*, 11211−11216.
Sugimoto, N., Nakano, S., Yoneyama, M., & Honda, K. (1996) *Nucl. Acids Res. 24*, 4501−4505.
Temsamani, J., Kubert, M., Tang, J. Y. Padmapriya, A., & Agrawal, S. (1994) *Antisense Res. Dev. 4*, 35−42.
Thierry, A. R., & Dritschilo, A. (1992) *Nucl. Acids Res. 20*, 5691−5698.
Vologodskii, A. V., Amirikyan, B. R., Lyubchenko, Y. L., & Frank-Kamenetskii, M. D. (1984) *J. Biomol. Struct. Dyn. 2*, 131−148.
Wagner, R. W. (1994) *Nature 372*, 333−335.
Zamecnik, P. C., & Stephenson, M. L. (1978) *Proc. Natl. Acad. Sci. U.S.A. 75*, 280−284.
Zimmerman, S. B., & Pheiffer, B. H. (1981) *Proc. Natl. Acad. Sci. U.S.A. 78*, 78−82.

BI9713557